A COMPREHENSIVE STUDY ON MECHANICAL PROPERTIES OF SLM PRINTED ALSI10MG ALLOY FOR VARIOUS PROCESS PARAMETERS

[1a] Suhas H Nayak,
[1b] Ranjith Kumar G S, [1c] Vijay Kumar S, [1d] Shiv Pratap SinghYadav, [1e] Kiran Aithal S, [1f] Nithin U Aithal

1[a, b, c, d, e, f], Department of Mechanical Engineering, Nitte Meenakshi Institute of Technology, Bangalore, India-560064.

Abstract: The use of aluminium (Al) metal components produced using selective laser melting (SLM) and additive manufacturing (AM) (SLM). Because of its unique qualities, such as high strength, stiffness to weight ratio, suitable formability, appropriate corrosion resistance, and recycling ability, aluminium is a good candidate to replace heavier materials (such as steel or copper) in the car and thus satisfy the demand for weight reduction in the automotive industry. New high strength aluminium alloys have been created as a consequence that are more compatible with the additive manufacturing (AM) process parameters, such as power (w), scan speed (m/s), and hatch distance (Hd). The alloy's mechanical properties are entirely influenced by the rate at which the component is heated and cooled. We also investigate the conventional methods for producing nanoporous anodic aluminium oxide, which include either gentle anodization or severe anodization. In this article, we provide a unique approach called "pulse anodization" that combines the benefits of moderate and hard anodization. By carefully adjusting the pulse sequences, it is possible to regulate the composition and pore structure of the anodic aluminium oxide films while still operating at a high throughput. The effects of adding magnesium and then heating the alloy are examined while it is slid against EN 24 steel. The alloy is a cast hypoeutectic aluminum-silicon alloy. By examining the morphology and chemistry of worn surface and subsurface, it is possible to identify the wear process. It was discovered that the stability of a mixed surface layer comprised of iron and aluminium was the main element determining wear resistance. All research is done using an SLM system with a 150W laser and a spot diameter of 50m. Following the tests, some intriguing data on the variations in alloys was found.

Keywords: Scan speed; Hatch distance; SLM; AM; Pulse sequences;

1. INTRODUCTION:

The modern developments in aluminium alloys for the automotive industry. Federal requirements require manufacturers to increase occupant safety and fuel economy while reducing exhaust pollutants. In order to meet this criterion, automakers are attempting to improve the efficiency of traditional engines, develop cutting-edge powertrains like hybrid systems, and lighter vehicles [1-3]. Weight reduction is crucial since it is projected that as a consequence of the auto industry's ongoing marketing of new models with better levels of luxury, convenience, performance, and protection in response to consumer demand, average vehicle weight will increase. According to general rules, a 10% weight reduction results in a 5.5% increase in fuel economy. By utilizing nanoporous anodic aluminum we can use the new technique of pulse anodization which has only the advantages of mild anodization and hard anodization because of the quick nature it can be widely used in the high valued industries [4-6]. By using this technique high output can be expected by controlling the pore structure of the anodic aluminum oxide and also composition of the element can also be controlled using the new pulse sequence. To increase the wear resistance of the material addition of magnesium was done for aluminum silicon alloy under heat treatment. In order to prove this the alloy was slid against a EN24 steel the slid particle surfaces were tested and it was found that upon addition of magnesium under heat treatment aluminum silicon alloy developed hardness in the surface which resulted in wear resistance.

2. METHODOLOGY

2.1 Chemical Composition of AlSi10Mg

Table 1: Chemical Composition of AlSi10Mg

Material Composition (weight %)		
Element	**Minimum**	**Maximum**
Aluminum	Remaining	
Silicon	9	11
Magnesium	0.20	0.45

2.2 Development of AlSi10Mg using Selective Laser Melting (SLM) Process

To produce items with intricate geometry or design Because it can print the item constructively layer by layer, selective laser melting (SLM) is among the most popular production methods. Because of this, there has been a lot of interest in modernizing the SLM process in recent years. Due of this, a lot of metal items are printed using the SLM technique, making it one of the major contributors to the metal additive manufacturing process. Derived from cutting-edge research on functional optimization and the development of novel techniques employing the SLM process [7-8]. Customized items are available and may be made of strong and lightweight materials such alloys of aluminium. Aluminum alloys have recently been mixed with silicone and magnesium to produce better components, even though the alloy was originally created using conventional casting methods.

In the initial stages of the selective laser melting process, metal powder is dispersed throughout the workspace and the build platform. A laser-generated heat source is then directed towards the powder on the build platform, tracing the predefined design or the geometry of the desired product as it melts the metal powder. The metal powder is targeted by the laser once the melt portion has once again solidified in order to print several layers of metal. When the desired density is attained, a piston in the system lowers the construction platform [9-12]. Up until the final product is made, the same procedure is used. Metal powder is cleared with a brush or pressurized air during the post-processing stage.

3. RESULTS AND DISCUSSIONS

3.1 Hardness Test

Table 3: Hardness Test Results

Sl/No	Sample No	P (W)	SS (mm/s)	D_h (mm)	Hardness (VHN)
1	Sample 1	100	200	0.05	189.5
2	Sample 2	100	300	0.07	184.1
3	Sample 3	100	400	0.09	178.2
4	Sample 4	150	200	0.07	194.5
5	Sample 5	150	300	0.09	191.3
6	Sample 6	150	400	0.05	175.4
7	Sample 7	200	200	0.09	169.2
8	Sample 8	200	300	0.05	171.8
9	Sample 9	200	400	0.07	180.8

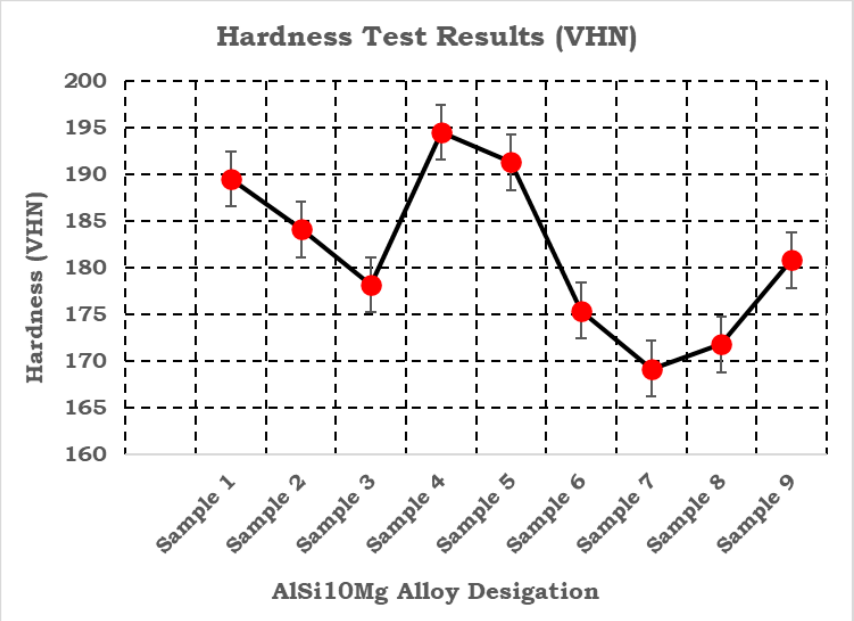

Figure 2: Hardness Test Results of AlSi10Mg

The Table 3 is used to tabulate and give the statistical value of the hardness test results of the AlSi10Mg alloy and in the figure 2 the same results are plotted using graphical method [13-14]. From the data we obtained we can observe that highest hardness is obtained at sample 4 that is for the input of 150Watts of power with scan speed of 200 millimeter per second with hatch distance of 0.07 millimeter for these inputs the highest output is obtained that is 194.5VHN. We can also determine the lowest hardness value which is obtained for sample 7 which has the input of 200watts of power with scan speed of 200 millimeter per second with a hatch distance of 0.09 millimeter per second which has lowest density of 169.2VHN. We can also determine the moderate hardness value that is around 177.5VHN.

Table 4: Experimental and Predicted Values of Hardness Test Results of AlSi10Mg

S/No	Sample No	Experimental	Predicted	Residual
1	Sample 1	189.50	188.629	0.87056
2	Sample 2	184.10	185.993	-1.89278
3	Sample 3	183.64	183.356	0.28389
4	Sample 4	182.54	183.679	-1.13944
5	Sample 5	181.44	181.043	0.39722
6	Sample 6	181.97	179.751	2.21889
7	Sample 7	180.21	178.729	1.48056
8	Sample 8	176.51	177.438	-0.92778
9	Sample 9	173.51	174.801	-1.29111

Table 4 indicate the Experimental and Predicted Values of Hardness test results of AlSi10Mg. Here, the experimental values are obtained using a software called Minitab and the predicted values are obtained by testing the components using Vickers hardness test equipment. The predicted values won't be accurate due to human error or machine error so the results are not so suggested. The residual here is the difference between the experimental values and the predicted values [15-16]. The highest difference between the experimental values and the predicted values is obtained for sample 6 whereas the lowest difference between the experimental values and the predicted values is obtained for sample 3.

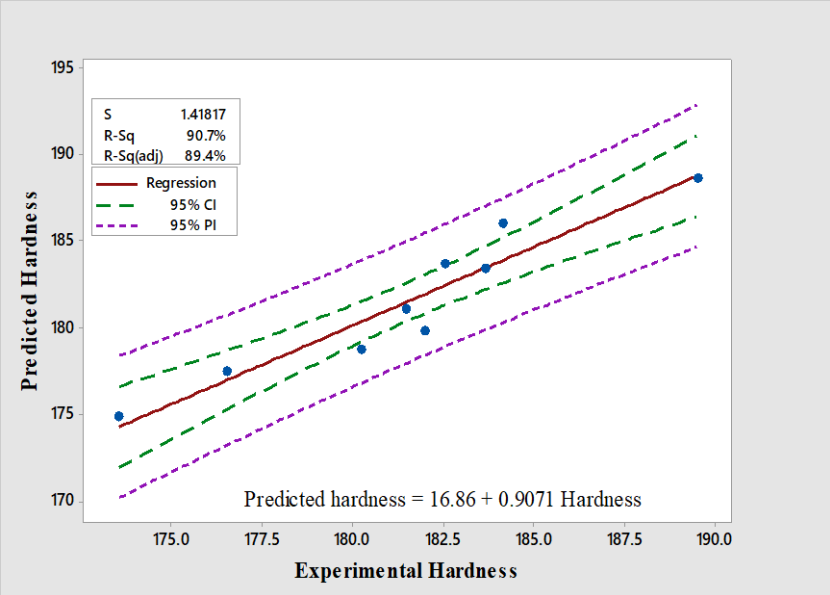

Figure 3: Predicted and Experimental Hardness for all combinations of AlSi10Mg

The Predicted and experimental hardness for all combinations of AlSi10Mg graph is plotted with predicted hardness against experimental hardness as shown in figure 3. The sample hardness is indicated as blue dots in the graph. The green and purple dotted lines are Predicted and experimental hardness values set at standard conditions [17-18]. The samples which come in these dotted lines are resulted as samples with less error and which are suitable. The samples which come out of those dotted lines are resulted in having more errors.

3.2 Regression Analysis of Hardness Values of AlSi10Mg:

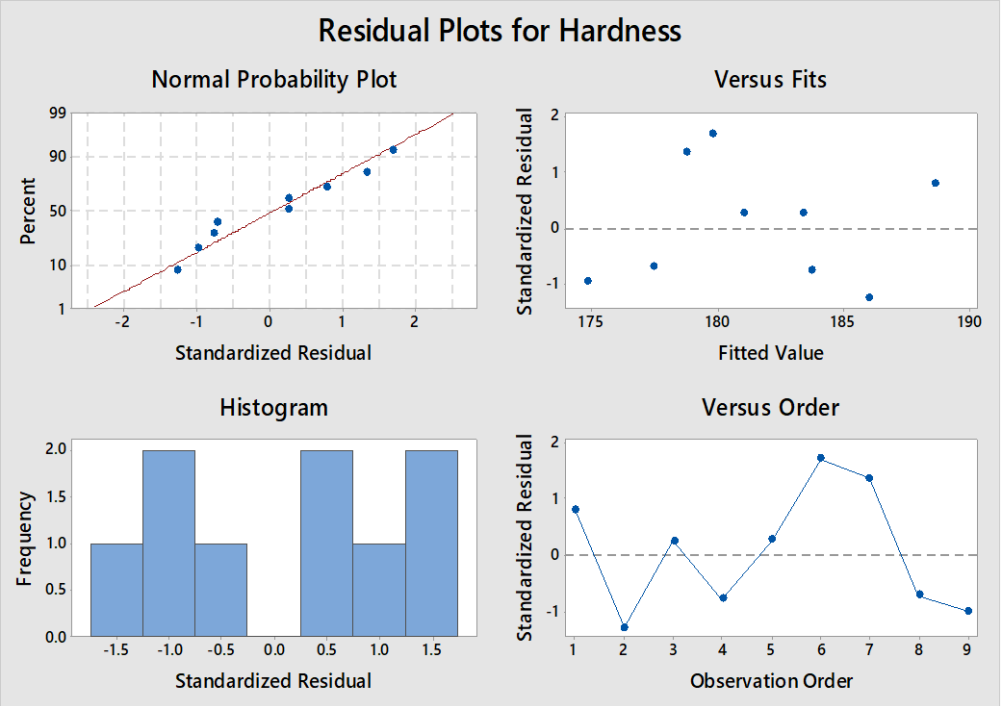

Figure 4: Normal Probability and Residual Plots of Hardness for all combinations considered

Regression analysis may be used to assess the connection between a based variable and one or more unbiased variables using a statistical method. It is also possible to determine how strongly the study's variables relate to one another, and this information may be used in the future to apply to these correlations.

CONCLUSION:

The article discussed about Using a selective laser melting approach, AlSi10Mg was successfully created by taking various process factors into account. The mechanical and microstructural characteristics of the composites were evaluated. The samples are listed with their respective hardness values and the results of a regression analysis of the hardness values of AlSi10Mg. Further the steps required to improve the mechanical properties of the alloy is also discussed. The article examines the most recent advancements made in Hoogovens's automobile industry's use of aluminium alloys. Hoogovens Aluminium is consistently enhancing the brazing alloys' performance in order to fulfil the market's expectations for lightweight constructions, as well as developing new generations of high strength alloys. With this goal in mind, Hoogovens Aluminium developed the Hogal-3572 and Hogal-3536 alloys, two new high strength/long-life alloys for CAB brazing. We talk about the current state and prospective futures of aluminium brazing sheet used in automotive applications. Special focus has been placed on the development of extended life alloys with enhanced corrosion performance in contrast to more traditional materials. The two processes that have historically been utilized to produce nanoporous anodic

aluminium oxide are mild anodization and hard anodization. The second method, widely employed in the aluminium industry, is quicker but produces films with disorganised pore patterns. The first method, which only produces self-ordered pore architectures under a limited set of processing conditions, is sluggish. Here we introduce "pulse anodization," a ground-breaking technique that combines the advantages of moderate and hard anodization. This study looked at how silicon and magnesium additions affected the development of the stage structure and microstructure of an additively manufactured aluminium alloy. AlSi10Mg that has undergone selective laser melting may also offer wear resistance that is equivalent to techniques used in the past. Fractures and subsequent particle compression into the floor force an agglomerated iron-rich floor layer upward. The abrasion and cracking of this layer produce particulate particles. The uniformity and equilibrium of this residue, the alloy's resistance to abrasion, which is governed by the base alloy's energy, and the shape of the second section debris all contribute to the determination of wear resistance. Magnesium is added to the matrix to reinforce it, and then the matrix is heated to further strengthen it and improve particle form. These treatments promote wear resistance by enhancing the floor layer's equilibrium and the base alloy's resistance to erosion.

Reference

1. W.S Miller, L Zhuang, J Bottema, A.J Wittebrood, P De Smet, A Haszler, A Vieregge (2000),” Recent development in aluminium alloys for the automotive industry” Materials Science and Engineering: A, Vol 280 (1), Pages 37-49, ISSN 0921-5093, https://doi.org/10.1016/S0921- 5093(99)00653-X.
2. Lee Woo, Schwirn Kathrin, Steinhart Martin, Pippel Eckhard, Scholz Roland, Gösele Ulrich, (2008), “Structural engineering of nanoporous anodic aluminium oxide by pulse anodization of aluminium”, Nature Nanotechnology, Vol-3 (4), ISSN: 1748-3395, https://doi.org/10.1038/nnano.2008.54.
3. Bai, B. P., & Biswas, S. K. (1991), “Effect of magnesium addition and heat treatment on mild wear of hypoeutectic aluminium-silicon alloys”, Acta metallurgica et materialia, Vol-39 (5), Pages 833-840, ISSN: 833-840, https://doi.org/10.1016/0956-7151(91)90283-7.
4. C. Bassi, M. Bloeck, R. Raiber, Erleichterter einsatz von aluminiumkarosserieblech imautomobil-grossserien durch trockenschmierstoffe, in: Proc. of Arbeitskreis Aluminium Automobil-Das Umformen von Aluminium im Automobilbau, Bad Nauheim, Germany, 20–21 May 1999, p. 92–105, 1999.
5. J. Bottema, C. Lahaye, R. Baartman, L. Zhuang, P. De Smet, Recent developments in AA6016-T4 aluminium type body sheet product, SAE Technical Paper Series 981007, 1998.
6. C.J. Miller, US Patents 3,321,828, May 30, 1967; 3,322,-517, May 30, 1967; 3,373,482, March 19, 1968; 3,373,482, March 19, 1968, assigned to General Electric Company.
7. N.D.A. Kooij, T.J. Hurd, A. Burger, K. Vieregge, A. HaszlerHigh strength heat-treatable aluminium alloys for CAB brazing, VTMS 4 Conf., London, UK, SAE Paper C543/014/99, 1999.
8. B. N. Pramila Bai and S. K. Biswas, ASLE Trans. 29, 116 (1986).
9. B. N. Pramila Bai, S. K. Biswas and N. N. Kumtekar, Wear 87, 237 (1983).
10. Kailas, S. V. (2020). Evolution of wear debris morphology during dry sliding of Ti–6Al–4V against SS316L under ambient and vacuum conditions. Wear, 456, 203378.
11. Poddar, P., Das, A., & Sahoo, K. L. (2014). Dry sliding wear characteristics of rheocast Mg–Sn based alloys. Materials & Design (1980-2015), 54, 820-830.
12. Jahangiri, M., Hashempour, M., Razavizadeh, H., & Rezaie, H. R. (2012). A new method to investigate the sliding wear behaviour of materials based on energy dissipation: W–25 wt% Cu composite. Wear, 274, 175-182.
13. Mahato, A., Verma, N., Jayaram, V., & Biswas, S. K. (2011). Severe wear of a near eutectic aluminium–silicon alloy. Acta Materialia, 59(15), 6069-6082.
14. Mahato, A., Xia, S., Perry, T., Sachdev, A., & Biswas, S. K. (2010). Role of silicon in resisting subsurface plastic deformation in tribology of aluminium–silicon alloys. Tribology International, 43(1-2), 381-387.
15. Wang, C. T., Gao, N., Wood, R. J., & Langdon, T. G. (2011). Wear behavior of an aluminum alloy processed by

equal-channel angular pressing. Journal of Materials Science, 46(1), 123-130.

16. Meghwal, A., Anupam, A., Schulz, C., Hall, C., Murty, B. S., Kottada, R. S., ... & Ang, A. S. M. (2022). Tribological and corrosion performance of an atmospheric plasma sprayed AlCoCr0. 5Ni high-entropy alloy coating. Wear, 506, 204443.

17. Deng, G., Chong, Y., Su, L., Zhan, L., Wei, P., Zhao, X., ... & Tsuji, N. (2022). Mechanisms of remarkable wear reduction and evolutions of subsurface microstructure and nano-mechanical properties during dry sliding of nano-grained Ti6Al4V alloy: A comparative study. Tribology International, 169, 107464.

18. Sert, Y., Küçükömeroğlu, T., Asl, H. G., & Göz, O. (2022). The Effect of Al and Ti Transition Metals on the Wear Resistance of Ceramic Based CrN Coatings; Investigation under Ambient Air and Vacuum Conditions. Proceedings of the Institution of Mechanical Engineers, Part L: Journal of Materials: Design and Applications, 236(3), 455-472.